THE EUROPEAN
PHYSICAL JOURNAL C

CrossMark

Charged-Higgs on $R_{D(*)}$, τ polarization, and FBA

Chuan-Hung Chen[1,a], **Takaaki Nomura**[2,b]

[1] Department of Physics, National Cheng-Kung University, Tainan 70101, Taiwan
[2] School of Physics, KIAS, Seoul 130-722, Korea

Abstract We study the influence of a charged-Higgs on the excess of branching fraction ratio, $R_M = BR(\bar{B} \to M\tau\bar{\nu}_\tau)/BR(\bar{B} \to M\ell\bar{\nu}_\ell)$ ($M = D, D^*$), in a generic two-Higgs-doublet model. In order to investigate the lepton polarization, the detailed decay amplitudes with lepton helicity are given. When the charged-Higgs is used to resolve excesses, it is found that two independent Yukawa couplings are needed to explain the R_D and R_{D^*} anomalies. We show that when the upper limit of $BR(B_c \to \tau\bar{\nu}_\tau) < 30\%$ is included, R_D can be significantly enhanced while $R_{D^*} < 0.27$. With the $BR(B_c \to \tau\bar{\nu}_\tau)$ constraint, we find that the τ-lepton polarizations can be still affected by the charged-Higgs effects, where the standard model (SM) predictions are obtained: $P_D^\tau \approx 0.324$ and $P_{D^*}^\tau \approx -0.500$, and they can be enhanced to be $P_D^\tau \approx 0.5$ and $P_{D^*}^\tau \approx -0.41$ by the charged-Higgs. The integrated lepton forward–backward asymmetry (FBA) is also studied, where the SM result is $\bar{A}_{FB}^{D^{(*)},\tau} \approx -0.359(0.064)$, and they can be enhanced (decreased) to be $\bar{A}_{FB}^{D^{(*)},\tau} \approx -0.33(0.02)$.

1 Introduction

The exclusive semileptonic $\bar{B} \to D^{(*)}\tau\bar{\nu}_\tau$ decay has drawn a lot of attention since the BaBar collaboration reported evidence for an excess in the ratio of branching ratios (BRs) [1,2], which is defined by

$$R_{D(*)} = \frac{BR(\bar{B} \to D^{(*)}\tau\bar{\nu})}{BR(\bar{B} \to D^{(*)}\ell\bar{\nu})}. \tag{1}$$

Intriguingly, a similar excess was also reported by Belle [3–5] and LHCb [6]. The averaged results from the heavy flavor averaging group (HFAG) now are given by [7]

$$R_D = 0.403 \pm 0.04 \pm 0.024,$$
$$R_{D^*} = 0.310 \pm 0.015 \pm 0.008, \tag{2}$$

where the standard model (SM) predictions are: $R_D^{\text{SM}} \approx 0.300$ [8,9] and $R_{D^*}^{\text{SM}} \approx 0.252$ [10]. Inspired by the unexpected measurements, many implications and speculations were studied in the literature [11–58].

In addition to the branching fraction ratio, Belle recently showed the measurement of τ polarization in the $\bar{B} \to D^*\tau\bar{\nu}_\tau$ decay:

$$P_{D^*}^\tau = \frac{\Gamma_{D^*}^{h=+} - \Gamma_{D^*}^{h=-}}{\Gamma_{D^*}^{h=+} + \Gamma_{D^*}^{h=-}} = -0.38 \pm 0.51^{+0.21}_{-0.16}, \tag{3}$$

where $\Gamma_{D^*}^\pm$ denotes the partial decay rate with a τ-lepton helicity of $h = \pm$, and the SM result is $P_{D^*}^\tau \approx -0.500$. Although the errors in the current observation are still large, any significant deviations from the SM results can indicate the new physics [18,62]. Based on the current experimental indications and from a phenomenological viewpoint, we investigate the impacts of a charged-Higgs on the semileptonic B decays in a generic two-Higgs-doublet model (THDM) [12,59,60].

Without imposing extra global symmetry, it is well known that the flavor-changing neutral currents (FCNCs) in the THDM can be induced at the tree level. The related couplings can be severely constrained by $\Delta F = 2$ processes, such as K–$\bar{K}$, B_q–$\bar{B}_q$ ($q = d, s$), and D–$\bar{D}$ mixings. However, these constraints occur in down-type quarks and the first two generations of up-type quarks. The top-quark-involving effects may not have serious bounds. Thus, with the constraints from the Higgs precision measurements, the BR for the $t \to ch$ process can be of the order of $10^{-4} - 10^{-3}$ [61]. It was found that the same FCNC coupling in the quark sector can help to resolve R_D and R_{D^*} excesses by the charged-Higgs mediation [12,59]. In addition, the tree-level FCNCs in the lepton sector not only can resolve the muon $g - 2$ anomaly, but also can provide a large BR to the lepton-flavor violating process,

such as $h \to \tau\mu$, for which the details can be found in our previous work [60].

In this study, we revisit the charged-Higgs Yukawa couplings to the $\bar{B} \to (D, D^*)\tau\nu_\tau$ processes in the generic THDM. In order to naturally suppress the FCNCs at the tree level, we adopt the so-called Cheng–Sher ansatz [63] in the quark and lepton sectors, where the Yukawa couplings are formulated by $Y_{ij} \propto \sqrt{m_i m_j}/v$. For the semileponic B decays, the main uncertainty is from the hadronic $\bar{B} \to D^{(*)}$ transition form factors. In order to restrain the influence of hadronic effects, we take the values of form factors so that the BRs for $\bar{B} \to D^{(*)}\ell\bar{\nu}_\ell$ ($\ell = e, \mu$) can fit the experimental data within 2σ errors. Although the charged-Higgs also contributes to the light lepton channels, due to the suppression of m_ℓ/v, its effects are small to the $\bar{B} \to D^{(*)}\ell\bar{\nu}_\ell$ decays. It is found that we need at least two new parameters to explain the R_D and R_{D^*} excesses; one is from quark sector, and the other is from the lepton sector. The conclusion is different from that shown in [12], in which only one parameter was required to explain the excesses. However, when the upper limit of $BR(B_c \to \tau\bar{\nu}_\tau) < 30\%$ obtained in [52,53] is taken into account, the allowed parameter space is strictly constrained. It will be seen that R_D can be significantly enhanced while the change of R_{D^*} is minor and can be only up to around 0.27.

In addition to the ratios of branching fractions, we also investigate the influence of the charged-Higgs on the lepton-helicity asymmetries, and lepton forward–backward asymmetries (FBAs). We find that τ polarizations in the $\bar{B} \to (D, D^*)\tau\bar{\nu}_\tau$ decays are sensitive to the charged-Higgs effects. For the FBA, the $\bar{B} \to D^*\tau\bar{\nu}_\tau$ process is more sensitive to the charged-Higgs effects.

The paper is organized as follows. In Sect. 2, we briefly introduce the charged Higgs Yukawa couplings to the quarks and leptons in the generic THDM. We formulate the decay amplitudes with the lepton-helicity states, the differential branching ratios, the lepton polarizations, and the lepton FBAs for $\bar{B} \to (D, D^*)\ell\bar{\nu}_\ell$ in Sect. 3. The numerical estimations and discussions are given in Sect. 4. A summary is shown in Sect. 5.

2 Charged-Higgs Yukawa Couplings in the THDM

To obtain the scalar couplings to the quarks and leptons in the model, the Yukawa sector is written as [60,68]

$$
\begin{aligned}
- \mathcal{L}_Y = {} & \bar{Q}_L Y_1^d D_R H_1 + \bar{Q}_L Y_2^d D_R H_2 \\
& + \bar{Q}_L Y_1^u U_R \tilde{H}_1 + \bar{Q}_L Y_2^u U_R \tilde{H}_2 \\
& + \bar{L} Y_1^\ell \ell_R H_1 + \bar{L} Y_2^\ell \ell_R H_2 + H.c.,
\end{aligned}
\tag{4}
$$

where the flavor indices are suppressed, $Q_L^T = (u, d)_L$ and $L^T = (\nu, \ell)_L$ are the $SU(2)_L$ quark and lepton doublets,

respectively, $Y_{1,2}^f$ are the Yukawa matrices, $\tilde{H}_2 = i\tau_2 H_2^*$ with $(i\tau_2)_{11(22)} = 0$ and $(i\tau_2)_{12(21)} = 1(-1)$, and the Higgs doublets are usually taken as

$$
H_i = \begin{pmatrix} \phi_i^+ \\ (v_i + \phi_i + i\eta_i)/\sqrt{2} \end{pmatrix}
\tag{5}
$$

with v_i being the VEV of H_i. Equation (4) can recover the type II THDM if $Y_2^{d,\ell}$ and Y_1^u vanish. Since ϕ_1 and ϕ_2 are two CP-even scalars, and they mix, we can introduce a mixing α angle to describe their physical states. The CP-odd and charged scalars are composed of $\eta_{1,2}$ and $\phi_{1,2}^\pm$, respectively; therefore, the mixing angle only depends on the ratio of v_1 and v_2. Hence, the relations between the physical and weak scalar states are expressed as

$$
\begin{aligned}
h &= -s_\alpha \phi_1 + c_\alpha \phi_2, \\
H &= c_\alpha \phi_1 + s_\alpha \phi_2, \\
H^\pm(A) &= -s_\beta \phi_1^\pm(\eta_1) + c_\beta \phi_2^\pm(\eta_2),
\end{aligned}
\tag{6}
$$

where h is the SM-like Higgs while H, A, and $H^\pm$ are new particles in the THDM, $c_\alpha(s_\alpha) = \cos\alpha(\sin\alpha)$, $c_\beta = \cos\beta = v_1/v$, and $s_\beta = \sin\beta = v_2/v$.

Using Eqs. (4) and (5), the quark and charged lepton mass matrices can be written as

$$
\mathbf{M}^f = \frac{v}{\sqrt{2}} \left(c_\beta Y_1^f + s_\beta Y_2^f \right).
\tag{7}
$$

We can diagonalize $\mathbf{M}^f$ by introducing unitary matrices V_L^f and V_R^f via $\mathbf{m}_{\text{dia}}^f = V_L^f \mathbf{M}^f V_R^{f\dagger}$. Accordingly, the charged Higgs Yukawa couplings to fermions can be found to be [60]

$$
\begin{aligned}
-\mathcal{L}_Y^{H^\pm} = {} & \sqrt{2}\bar{d}_L \mathbf{V}^\dagger \left[-\frac{\cot\beta}{v}\mathbf{m_u} + \frac{\mathbf{X}^u}{s_\beta} \right] u_R H^- \\
& + \sqrt{2}\bar{u}_L \mathbf{V} \left[-\frac{\tan\beta}{v}\mathbf{m_d} + \frac{\mathbf{X}^d}{c_\beta} \right] d_R H^+ \\
& + \sqrt{2}\bar{\nu}_L \left[-\frac{\tan\beta}{v}\mathbf{m}_\ell + \frac{\mathbf{X}^\ell}{c_\beta} \right] \ell_R H^+ + H.c.,
\end{aligned}
\tag{8}
$$

where $\mathbf{V}$ denotes the Cabibbo–Kobayashi–Maskawa (CKM), and $\mathbf{X^f}$ is defined by

$$
\mathbf{X^u} = V_L^u \frac{Y_1^u}{\sqrt{2}} V_R^{u\dagger}, \quad \mathbf{X^d} = V_L^d \frac{Y_2^d}{\sqrt{2}} V_R^{d\dagger}, \quad \mathbf{X^\ell} = V_L^\ell \frac{Y_2^\ell}{\sqrt{2}} V_R^{\ell\dagger}.
\tag{9}
$$

From Eq. (8), it can be seen that X_{ij}^f dictates not only FCNCs but also violation of lepton universality; in addition, the effects of X^d and X^ℓ can be further enhanced with a large value of $\tan\beta$, i.e., $c_\beta \ll 1$. Although the Y_1^f and Y_2^f Yukawa matrices basically are arbitrary free parameters, since they are related to the fermion masses, in order to show the mass-dependence effects, we further adopt the Cheng–Sher ansatz

for X_{ij}^f as $X_{ij}^f = \sqrt{m_i^f m_j^f}/v\, \chi_{ij}^f$ [63], where X_{ij}^f now are suppressed by $\sqrt{m_i^f m_j^f}/v$, and χ_{ij}^f are the free parameters.

Before we further discuss the effective interactions mediated by the charged Higgs for the $b \to c\ell\bar{\nu}_\ell$ process, we analyze the effect of $\mathbf{X}^u$ associated with the CKM matrix, such as $(\mathbf{V}^\dagger \mathbf{X}^u)_{bc}$ in Eq. (8). If we assume that $\mathbf{X}^u$ is a diagonal matrix, it can be clearly seen that $(\mathbf{V}^\dagger \mathbf{X}^u)_{bc} = V_{cb}^* X_{cc}^u$. With the Cheng–Sher ansatz, the charged Higgs Yukawa couplings are then suppressed by m_c/v. Due to the fact that there is no significant $\tan\beta$ enhancement, the contribution is expected to be small. However, if X_{ij}^u with $i \neq j$ are allowed, $(\mathbf{V}^\dagger \mathbf{X}^u)_{bc}$ can be simplified as

$$(\mathbf{V}^\dagger \mathbf{X}^u)_{bc} = V_{ub}^* X_{uc}^u + V_{cb}^* X_{cc}^u + V_{tb}^* X_{tc}^u,$$
$$\approx \frac{\sqrt{m_t m_c}}{v} \chi_{tc}^u, \tag{10}$$

where we have taken $|V_{ub}| < |V_{cb}| \ll V_{tb} \approx 1$ and the Cheng–Sher relation. With the approximation $\sqrt{m_t m_c}/v \sim V_{cb}$, it can be seen that $\chi_{tc}^u \sim O(1)$ indicates a large coupling at the b–c–$H^\pm$ vertex and could help to resolve the excesses. A similar situation also occurs in the $(\mathbf{V}\mathbf{X}^d)_{cb}$, which can be expressed as $(\mathbf{V}\mathbf{X}^d)_{cb}/c_\beta \approx \sqrt{m_b m_s} \chi_{sb}^d/v$. Since χ_{sb}^d can be limited by the $\Delta B = 2$ process via the mediation of neutral scalar bosons at the tree level, we can ignore its contribution. Hence, we focus on the influence of χ_{tc}^u.

3 Phenomenological formulations

Combining the SM and $H^\pm$ contributions, the effective Hamiltonian for $b \to c\ell\bar{\nu}_\ell$ is written as

$$H_{\text{eff}} = \frac{G_F}{\sqrt{2}} V_{cb} \Big[(\bar{c}b)_{V-A}(\bar{\ell}\nu)_{V-A}$$
$$+ C_L^\ell (\bar{c}b)_{S-P}(\bar{\ell}\nu)_{S-P} + C_R^\ell (\bar{c}b)_{S+P}(\bar{\ell}\nu)_{S-P} \Big], \tag{11}$$

where $(\bar{f}'f)_{V\pm A} = \bar{f}'\gamma^\mu(1\pm\gamma_5)f$, $(\bar{f}'f)_{S\pm P} = \bar{f}'(1\pm\gamma_5)f$, and the coefficients from the charged Higgs with $g^2/(8m_W^2) = 1/(2v^2)$ are given by

$$C_L^\ell \approx -\frac{m_c m_\ell}{m_{H^\pm}^2}\left(1 - \frac{\chi_{\ell\ell}^\ell}{s_\beta}\right)\left(1 - \sqrt{\frac{m_t}{m_c}}\frac{\chi_{ct}^u}{c_\beta V_{cb}}\right), \tag{12}$$

$$C_R^\ell \approx -\frac{m_b m_\ell \tan^2\beta}{m_{H^\pm}^2}\left(1 - \frac{\chi_{\ell\ell}^\ell}{s_\beta}\right). \tag{13}$$

It can be seen that without $\chi_{\ell\ell}^\ell$ and χ_{ct}^u, both C_L^ℓ and C_R^ℓ are negative and correspond to the type-II THDM; as a result, they are destructive contributions to the SM [1]. In addition to the sign issue, we also need to adjust $C_R^\ell + C_L^\ell$ and $C_R^\ell - C_L^\ell$ so that R_D and R_{D^*} can be explained at the same time. In order to

demonstrate the effects of the generic THDM, we will discuss the situations with and without $\chi_{\ell\ell}^\ell$ and χ_{ct}^u after we introduce the differential decay rates for the $\bar{B} \to (D, D^*)\ell\bar{\nu}_\ell$ decays.

To calculate the exclusive semileptonic B decays, we parametrize the $B \to (D, D^*)$ transition form factors as

$$\langle D(p_2)|\bar{c}\gamma^\mu b|\bar{B}(p_1)\rangle = F_1(q^2)\left[P^\mu - \frac{P\cdot q}{q^2}q^\mu\right]$$
$$+ F_0(q^2)\frac{P\cdot q}{q^2}q^\mu,$$
$$\langle D(p_2)|\bar{c}b|\bar{B}(p_1)\rangle = (m_B + m_D)F_S(q^2), \tag{14}$$

$$\langle D^*(p_2,\epsilon)|\bar{c}\gamma^\mu b|\bar{B}(p_1)\rangle = \frac{V(q^2)}{m_B + m_{D^*}}\epsilon^{\mu\nu\rho\sigma}\epsilon_\nu^* P_\rho q_\sigma,$$
$$\langle D^*(p_2,\epsilon)|\bar{c}\gamma^\mu\gamma_5 b|\bar{B}(p_1)\rangle$$
$$= 2im_{D^*}A_0(q^2)\frac{\epsilon^*\cdot q}{q^2}q^\mu + i(m_B + m_{D^*})A_1(q^2)$$
$$\times\left[\epsilon_\mu^* - \frac{\epsilon^*\cdot q}{q^2}q^\mu\right] - iA_2(q^2)\frac{\epsilon^*\cdot q}{m_B + m_{D^*}}$$
$$\times\left[P^\mu - \frac{P\cdot q}{q^2}q^\mu\right],$$
$$\langle D^*(p_2,\epsilon)|\bar{c}\gamma_5 b|\bar{B}(p_1)\rangle = -i\epsilon^*\cdot q\, F_P(q^2), \tag{15}$$

where $\epsilon^{0123} = 1$, $P = p_1 + p_2$, $q = p_1 - p_2$; ϵ is the polarization vector of D^* meson, and $\epsilon\cdot\epsilon^* = -1$. Using the equations of motion $i\slashed{\partial}b = m_b b$ and $\bar{c}i\slashed{\partial} = -m_c\bar{c}$, we obtain the relationships

$$F_S(q^2) \approx \frac{m_B - m_D}{m_b(\mu) - m_c(\mu)}F_0(q^2),$$
$$F_P(q^2) \approx \frac{2m_{D^*}}{m_b(\mu) + m_c(\mu)}A_0(q^2), \tag{16}$$

where $m_{b,c}(\mu)$ are the current quark masses at the μ scale. According to the interactions in Eq. (11), the decay amplitudes for $\bar{B} \to (D, D^*)\ell\bar{\nu}_\ell$ are then

$$A_D = \frac{G_F}{\sqrt{2}}V_{cb}\Big[F_1\Big(P^\mu - \frac{P\cdot q}{q^2}q^\mu\Big)(\bar{\ell}\nu)_{V-A}$$
$$+ \Big(m_\ell F_0\frac{P\cdot q}{q^2} + (C_R^\ell + C_L^\ell)(m_B + m_D)F_S\Big)(\bar{\ell}\nu)_{S-P}\Big],$$
$$A_{D^*}^L = -i\frac{G_F}{\sqrt{2}}V_{cb}\Big\{\epsilon^*\cdot q\Big((C_R^\ell - C_L^\ell)F_P + 2A_0\frac{m_{D^*}m_\ell}{q^2}\Big)(\bar{\ell}\nu)_{S-P}$$
$$+ \Big[(m_B + m_{D^*})A_1\Big(\epsilon_\mu^*(L) - \frac{\epsilon^*\cdot q}{q^2}q_\mu\Big)$$
$$- \frac{A_2\epsilon^*\cdot q}{m_B + m_D}\Big(P_\mu - \frac{P\cdot q}{q^2}q_\mu\Big)\Big](\bar{\ell}\nu)_{V-A}\Big\},$$
$$A_{D^*}^T = \frac{G_F}{\sqrt{2}}V_{cb}\Big[\frac{V}{m_B + m_{D^*}}\varepsilon_{\mu\nu\rho\sigma}\epsilon_\nu^*(T)P^\rho q^\sigma$$
$$- i(m_B + m_{D^*})A_1\epsilon_\mu^*(T)\Big](\bar{\ell}\nu)_{V-A}, \tag{17}$$

where we have suppressed the q^2-dependence in the form factors, and $A_{D^*}^L$ and $A_{D^*}^T$ denote the longitudinal and transverse components of D^*-meson, respectively. It can be seen that the charged Higgs only affects the longitudinal part.

In order to derive the differential decay rate with a specific lepton helicity, we set the coordinates of various kinematic variables in the rest frame of $\ell\bar{\nu}$ invariant mass as

$$q = (\sqrt{q^2}, 0, 0, 0), \ p_M = (E_M, 0, 0, p_M),$$

$$E_M = \frac{1}{2\sqrt{q^2}}(m_B^2 - q^2 - m_M^2), \tag{18}$$

$$p_M = \frac{\sqrt{\lambda_M}}{2\sqrt{q^2}},$$

$$p_\nu = (E_\nu, p_\nu \sin\theta_\ell \cos\phi, p_\nu \sin\theta_\ell \sin\phi, p_\nu \cos\theta_\ell),$$

$$p_\ell = (E_\ell, -\mathbf{p}_\nu),$$

$$\epsilon(L) = \frac{1}{m_{D^*}}(p_{D^*}, 0, 0, E_{D^*}), \ \epsilon(\pm)$$

$$= \frac{1}{\sqrt{2}}(0, \mp 1, -i, 0), \ p_\ell = p_\nu = \frac{q^2 - m_\ell^2}{2\sqrt{q^2}}, \tag{19}$$

where θ_ℓ is the polar angle of a neutrino with respect to the moving direction of M meson in the q^2 rest frame, and the components of $\vec{p}_\ell$ can be obtained from $\vec{p}_\nu$ by using $\pi - \theta_\ell$ and $\phi + \pi$ instead of θ_ℓ and ϕ. Since the SM neutrino is left-handed, if we neglect its small mass, its helicity can be fixed to be negative; therefore, we focus on the helicity amplitudes of a charged lepton. Accordingly, the charged lepton-helicity amplitudes for the $\bar{B} \to D\ell\bar{\nu}_\ell$ decay can be derived as

$$A_D^{L,h=+} = \frac{G_F V_{cb}}{\sqrt{2}}\left(2m_\ell\beta_\ell\frac{\sqrt{\lambda_D}}{\sqrt{q^2}}F_1\cos\theta_\ell - 2\beta_\ell\sqrt{q^2}X_D^{0\ell}\right), \tag{20}$$

$$A_D^{L,h=-} = \frac{G_F V_{cb}}{\sqrt{2}}\left(-2\beta_\ell\sqrt{\lambda_D}F_1\sin\theta_\ell\right), \tag{21}$$

$$X_D^{0\ell} = \frac{m_B^2 - m_D^2}{q^2}m_\ell F_0 + (m_B + m_D)\left(C_R^\ell + C_L^\ell\right)F_S, \tag{22}$$

where $\beta_\ell = (1 - m_\ell^2/q^2)^{1/2}$, $h = +(-)$ denotes the positive (negative) helicity of a charged lepton, and the detailed spinor states and derivations of $(\bar{\ell}\nu)_{V-A}$ and $(\bar{\ell}\nu)_{S-P}$ with polarized leptons are given in the appendix. Although the D meson does not carry spin degrees of freedom, in order to use similar notation to that in the $\bar{B} \to D^*\ell\bar{\nu}_\ell$ decay, we put an extra index L in $A_D^{L,h=\pm}$.

With the same approach, we can obtain the helicity amplitudes for the $\bar{B} \to D^*\ell\bar{\nu}_\ell$ decay. Since the D^* meson is a vector boson and carries spin degrees of freedom, we separate the lepton-helicity amplitudes into longitudinal (L) and transverse (T) parts to show the information for each D^* polarization. Thus, the helicity amplitudes for $\bar{B} \to D^*\ell\bar{\nu}_\ell$ with the D^* longitudinal polarization are found to be

$$A_{D^*}^{L,h=+} = -i\frac{G_F V_{cb}}{\sqrt{2}}\left(2m_\ell\beta_\ell h_{D^*}^0\cos\theta_\ell - 2\beta_\ell\frac{\sqrt{\lambda_{D^*}}}{\sqrt{q^2}}X_{D^*}^{0\ell}\right), \tag{23}$$

$$A_{D^*}^{L,h=-} = -i\frac{G_F V_{cb}}{\sqrt{2}}\left(-2\sqrt{q^2}\beta_\ell h_{D^*}^0\sin\theta_\ell\right), \tag{24}$$

$$h_{D^*}^0(q^2) = \frac{1}{2m_{D^*}\sqrt{q^2}}\left[(m_B^2 - m_{D^*}^2 - q^2)(m_B + m_{D^*})A_1\right.$$

$$\left. - \frac{\lambda_{D^*}}{m_B + m_{D^*}}A_2\right],$$

$$X_{D^*}^{0\ell} = m_\ell A_0 + \frac{q^2}{2m_D^*}(C_R^\ell - C_L^\ell)F_P. \tag{25}$$

It can be seen that the formulas of $A_{D^*}^{L,h=\pm}$ are similar to those of $A_D^{L,h=\pm}$. The decay amplitudes with the D^* transverse polarizations are given by

$$A_{D^*}^{T=\pm,h=+} = i\frac{G_F V_{cb}}{\sqrt{2}}\left[-\sqrt{2}m_\ell\beta_\ell\sin\theta_\ell e^{\mp i\phi}\right]h_{D^*}^\pm, \tag{26}$$

$$A_{D^*}^{T=\pm,h=-} = \mp i\frac{G_F V_{cb}}{\sqrt{2}}\left[-\sqrt{2}\sqrt{q^2}\beta_\ell(1\mp\cos\theta_\ell)e^{\mp i\phi}\right]h_{D^*}^\pm, \tag{27}$$

$$h_{D^*}^\pm = \frac{\sqrt{\lambda_{D^*}}}{m_B + m_{D^*}}V \mp (m_B + m_{D^*})A_1.$$

Since the scalar charged Higgs cannot affect the transverse parts, the $A_{D^*}^{T=\pm,h=\pm}$ are only from the SM contributions. According to these helicity amplitudes, it can be clearly seen that due to angular-momentum conservation, the $A_D^{L,h=+}$ and $A_{D^*}^{L(T),h=+}$, which come from $\bar{\ell}\gamma_\mu(1 - \gamma_5)\nu$, are chiral suppression and proportional to m_ℓ. The charged lepton in $\bar{\ell}(1 - \gamma_5)\nu$ prefers the $h = +$ state and in principle has no chiral suppression; however, in our case, chiral suppression exists and is from the charged-Higgs Yukawa couplings due to the Cheng–Sher ansatz.

Including the three-body phase space, the differential decay rates with lepton helicity and D^* polarization as a function of q^2 and $\cos\theta_\ell$ can be obtained:

$$\frac{d\Gamma_D^{h=\pm}}{dq^2 d\cos\theta_\ell} = \frac{\sqrt{\lambda_D}}{512\pi^3 m_B^3}\beta_\ell^2|A_D^{L,h=\pm}|^2,$$

$$\frac{d\Gamma_{D^*}^{L(T),h=\pm}}{dq^2 d\cos\theta_\ell} = \frac{\sqrt{\lambda_{D^*}}}{512\pi^3 m_B^3}\beta_\ell^2|A_{D^*}^{L(T),h=\pm}|^2. \tag{28}$$

The differential decay rates, which integrate out the polar θ_ℓ angle, are shown in the appendix. In addition to the branching fraction ratios R_D and R_{D^*}, based on Eq. (28), we can also study the lepton-helicity asymmetry [13,18,62] (see also Refs. [64,65]) and the FBA [66,67]. Helicity asymmetry can be defined by

$$P_M^\ell = \frac{\Gamma_M^{h=+} - \Gamma_M^{h=-}}{\Gamma_M^{h=+} + \Gamma_M^{h=-}}, \tag{29}$$

where $M = D, D^*$ and $\Gamma_{D^*}^{h=\pm} = \sum_{\lambda=L,\pm} \Gamma_{D^*}^{\lambda,h=\pm}$ have summed all D^* polarizations. From Eqs. (51) and (53), the lepton-helicity asymmetries for $\bar{B} \to (D, D^*)\ell\bar{\nu}_\ell$ with charged Higgs effects can be found to be

$$P_D^\ell = \frac{\int_{m_\ell^2}^{q_{\max}^2} dq^2 \sqrt{\lambda_D} \beta_\ell^4 \left[\frac{2}{3}(m_\ell^2 - 2q^2)\lambda_D F_1^2/q^2 + 2m_\ell^2 q^2 |X_D^{0\ell}|^2 \right]}{\int_{m_\ell^2}^{q_{\max}^2} dq^2 \sqrt{\lambda_D} \beta_\ell^4 \left[\frac{2}{3}(m_\ell^2 + 2q^2)\lambda_D F_1^2/q^2 + 2m_\ell^2 q^2 |X_D^{0\ell}|^2 \right]}, \tag{30}$$

$$P_{D^*}^\ell = \frac{\int_{m_\ell^2}^{q_{\max}^2} dq^2 \sqrt{\lambda_{D^*}} \beta_\ell^4 \left[\frac{2}{3}(m_\ell^2 - 2q^2)\left(\sum_{\lambda=L,\pm} |h_{D^*}^\lambda|^2\right) + 2(m_\ell^2/q^2)\lambda_{D^*}|X_{D^*}^{0\ell}|^2 \right]}{\int_{m_\ell^2}^{q_{\max}^2} dq^2 \sqrt{\lambda_{D^*}} \beta_\ell^4 \left[\frac{2}{3}(m_\ell^2 + 2q^2)\left(\sum_{\lambda=L,\pm} |h_{D^*}^\lambda|^2\right) + 2(m_\ell^2/q^2)\lambda_{D^*}|X_{D^*}^{0\ell}|^2 \right]}. \tag{31}$$

The lepton FBA can be defined by

$$A_{FB}^{M,\ell}(q^2) = \frac{\int_0^1 dz(d\Gamma_M/dq^2 dz) - \int_{-1}^0 dz(d\Gamma_M/dq^2 dz)}{\int_0^1 dz(d\Gamma_M/dq^2 dz) + \int_{-1}^0 dz(d\Gamma_M/dq^2 dz)}, \tag{32}$$

where $z = \cos\theta_\ell$, and Γ_M denotes the total partial decay rate for the $\bar{B} \to M\ell\bar{\nu}_\ell$ decay. Accordingly, the FBAs mediated by the charged Higgs and W-boson in $\bar{B} \to (D, D^*)\ell\bar{\nu}_\ell$ are obtained:

$$A_{FB}^{D,\ell}(q^2) = -\frac{2m_\ell\sqrt{\lambda_D}F_1 X_D^0}{H_D^+ + H_D^-},$$
$$A_{FB}^{D^*,\ell}(q^2) = \frac{1}{\sum_{\lambda=L,\pm}(H_{D^*}^{\lambda,+} + H_{D^*}^{\lambda,-})}$$
$$\times \left[-2m_\ell \frac{\sqrt{\lambda_{D^*}}}{\sqrt{q^2}} h_{D^*}^0 X_{D^*}^0 + 4q^2 \sqrt{\lambda_{D^*}} A_1 V \right]. \tag{33}$$

From Eq. (33), it can be seen that the FBAs in the $A_{FB}^{D,\ell}$ and the longitudinal part of $A_{FB}^{D^*,\ell}$ depend on m_ℓ and are chiral suppressed. Due to $m_\tau/m_b \sim 0.4$, which is not highly suppressed, we expect $\bar{B} \to D\tau\bar{\nu}_\tau$ to have a sizable FBA. Moreover, since $A_{FB}^{D^*,\ell}$ does not vanish in the chiral limit, it can be sizable in a light charged lepton mode. Basically, the observations of the tau polarization and FBA rely on tau-lepton reconstruction, where the kinematic information is from its decay products; however, since the final state in a tau decay at least involves one invisible neutrino, it is experimentally challenging to measure the polarization and FBA. Instead of a τ reconstruction, an approach using the kinematics of visible particles in τ decays has recently been proposed by

the authors in [69], where the tau polarization and FBA can be extracted from an angular asymmetry of visible particles in a tau decay. Accordingly, it is shown that the $\tau \to \pi\nu_\tau$ decay is the most sensitive channel. Based on this new approach, a statistical precision of 10% can be achieved at Belle II with an integrated luminosity of 50 ab^{-1}. The detailed analysis can be found in [69].

4 Numerical analysis and discussions

4.1 Roles of the $\chi_{\tau\tau}^\ell$ and χ_{ct}^u parameters

Before presenting the detailed numerical analysis, we first discuss the influence of $\chi_{\ell\ell}^\ell$ and χ_{ct}^u on the C_R^ℓ and C_L^ℓ. From Eqs. (22) and (25), it can be seen that the $\bar{B} \to (D, D^*)\ell\bar{\nu}_\ell$ decays are related to $C_R^\ell + C_L^\ell$ and $C_R^\ell - C_L^\ell$, respectively. If the charged-Higgs can resolve the anomalies, the main effects then are on the $\tau\bar{\nu}_\tau$ modes due to the lepton mass-dependent Yukawa couplings. In the following study, we concentrate on the $\bar{B} \to (D, D^*)\tau\bar{\nu}_\tau$ decays. Since the measured R_D and R_{D^*} are somewhat higher than the SM predictions, the $H^\pm$ effects should constructively interfere with the SM contributions. Thus, we have to require $C_R^\tau \pm C_L^\tau > 0$. Furthermore, from Eq. (23), the charged-Higgs contribution is associated with the $\sqrt{\lambda_{D^*}}$ factor, which represents $|\vec{p}_{D^*}|$ and decreases while q^2 increases; as a result, the $H^\pm$ effects on the $BR(\bar{B} \to D^*\tau\bar{\nu}_\tau)$ are not as sensitive as those on the $BR(\bar{B} \to D\tau\bar{\nu}_\tau)$. Therefore, to simultaneously enhance R_D and R_{D^*} through the mediation of the charged-Higgs, we conclude $C_R^\tau - C_L^\tau > C_R^\tau + C_L^\tau > 0$; that is, $C_R^\tau > 0 > C_L^\tau$. We note that $C_{R,L}^\ell$ from other scalar boson can in general be much larger than the SM contributions, so the interference effects are not important. Since the $H^\pm$ couplings are proportional to the $m_\ell \tan\beta/v$, even with a large $\tan\beta$ case, the effects are naturally limited. Hence, our discussions can be only applied to the charged-Higgs-like case.

Following the analysis above, we now discuss the roles of $\chi_{\tau\tau}^\ell$ and χ_{ct}^u in the C_R^τ and C_L^τ. From Eq. (13), it can be seen that without $\chi_{\tau\tau}^\ell$, $C_R^\tau < 0$. In other words, we need $\chi_{\tau\tau}^\ell$ to tune the sign of C_R^τ from negative to positive. According to Eq. (12), if we take $C_R^\tau > 0$ and ignore the χ_{ct}^u factor, the sign of C_L^τ is positive, which disfavors our earlier conclusion. Hence, we need χ_{ct}^u to flip the positive C_L^τ to make it
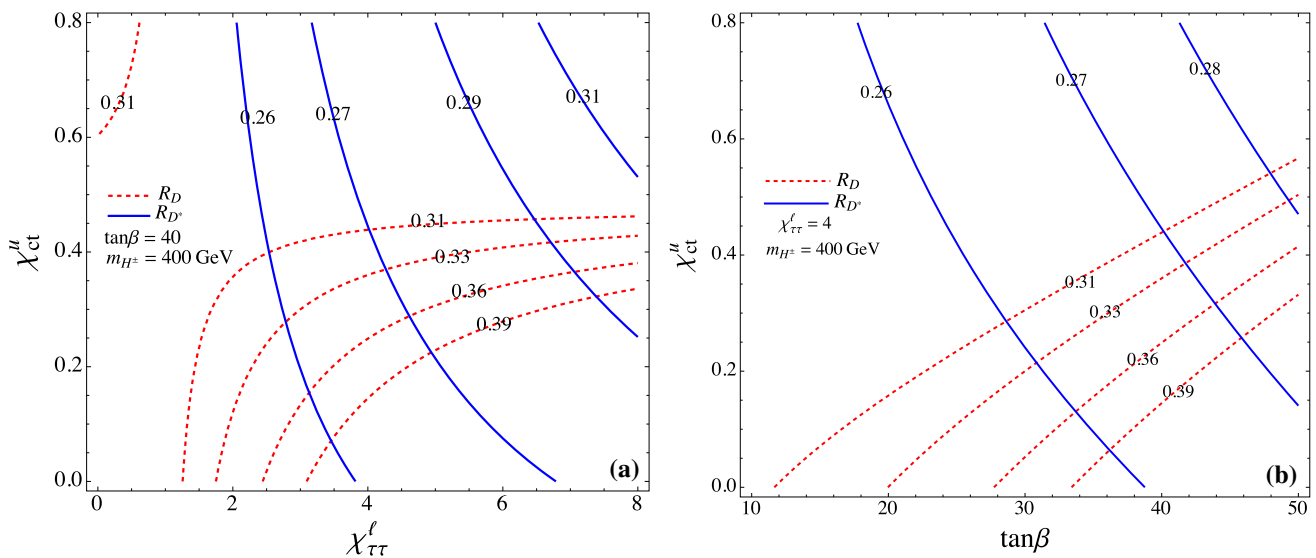
Fig. 1 Contours for R_D (dashed) and R_{D^*} (solid) as a function of χ_{ct}^u and **a** $\chi_{\tau\tau}^\ell$ with $\tan\beta = 40$, **b** $\tan\beta$ with $\chi_{\tau\tau}^\ell = 4$, where we have fixed $m_{H^\pm} = 400$ GeV

negative. In addition to the signs of C_R^τ and C_L^τ, their magnitudes are also an important issue. The charged-Higgs Yukawa couplings generally depend on the fermion mass, with the exception of the top-quark, and the couplings are suppressed by the m_f/v. To enhance the involved Yukawa couplings, we adopt a scenario with a large value of $\tan\beta$.

4.2 Numerical analysis of $R_{D^{(*)}}$ and constraint from $B_c \to \tau\bar{\nu}_\tau$

To estimate the physical quantities of the exclusive semileptonic B decays, we use the $B \to M$ form factors, which were calculated based on the heavy quark effective theory (HQET) and shown in [22,70]. The corrections of $\mathcal{O}(\Lambda_{QCD}/m_{b,c})$ and $\mathcal{O}(\alpha_s)$ to the form factors can be found in [71]. Most phenomena of interest in this work are related to the ratios of squared decay amplitudes, where V_{cb} is canceled and the influence from the uncertainties of form factors is mild. In order to fix the parameters in the $B \to M$ transition form factors, we adopt the parameter values of the form factors so that the BRs for $\bar{B} \to (D, D^*)\ell\bar{\nu}_\ell$ in the SM satisfy the experimental data within 1σ errors. With $V_{cb} = 3.93 \times 10^{-2}$ and the form factors in [22,70], we get the BRs for $B^- \to D^{(*)}\ell\bar{\nu}_\ell$ in the SM as

$$BR(B^- \to D\ell\bar{\nu}_\ell) \approx 2.26\,[2.16]\%\ \text{HQET [RQM]},$$
$$BR(B^- \to D^*\ell\bar{\nu}_\ell) \approx 5.58\,[5.81]\%\ \text{HQET [RQM]}, \quad (34)$$

where the experimental data are $BR^{\exp}(B^- \to D\ell\bar{\nu}_\ell) = (2.27 \pm 0.11)\%$ and $BR^{\exp}(B^- \to D^*\ell\bar{\nu}_\ell) = (5.69 \pm 0.19)\%$ [73]. For comparison, we also show the results using the form factors calculated in the framework of relativistic quark models (RQM) [72]. Using the same values of V_{cb} and

form factors, the BRs for $B^- \to (D, D^*)\tau\nu_\tau$ in the SM can be straightforwardly calculated to be

$$BR(B^- \to D\tau\bar{\nu}_\tau) \approx 0.69\,[0.63]\%\ \text{HQET [RQM]},$$
$$BR(B^- \to D^*\tau\bar{\nu}_\tau) \approx 1.43\,[1.42]\%\ \text{HQET [RQM]}, \quad (35)$$

where the experimental values are $BR^{\exp}(B^- \to D\tau\bar{\nu}_\tau) = (0.77 \pm 0.25)\%$ and $BR^{\exp}(B^- \to D^*\tau\bar{\nu}_\tau) = (1.88 \pm 0.20)\%$ [73]. It can be seen that the $\tau\bar{\nu}_\tau$ measurements are somewhat larger than the theoretical estimations. The resulting ratios R_D and R_{D^*} and tau polarizations in the SM are given by

$$R_D \approx 0.307, \quad R_{D^*} \approx 0.257, \quad (36)$$
$$P_D^{\tau(\mu)} \approx 0.324(-0.962), \quad P_{D^*}^{\tau(\mu)} \approx -0.513(-0.986). \quad (37)$$

The obtained values of R_{D,D^*} are close to those values shown in [8–10]. We will use the form factors to estimate the τ polarizations and FBAs.

In order to present the charged-Higgs influence on the ratios R_{D,D^*}, we adopt the formulas parametrized as [10]

$$R_D \approx R_D^{SM}\left[1 + 1.5Re(C_R^\tau + C_L^\tau) + 1.0|C_R^\tau + C_L^\tau|^2\right], \quad (38)$$
$$R_{D^*} \approx R_{D^*}^{SM}\left[1 + 0.12Re(C_R^\tau - C_L^\tau) + 0.05|C_R^\tau - C_L^\tau|^2\right]. \quad (39)$$

Accordingly, we show the contours for R_D and R_{D^*} as a function of $\chi_{\tau\tau}^\ell$ and χ_{ct}^u in Fig. 1(a) and of $\tan\beta$ and χ_{ct}^u in Fig. 1(b), where we fix $\tan\beta = 40$ and $\chi_{\tau\tau}^\ell = 4$ in the plots,
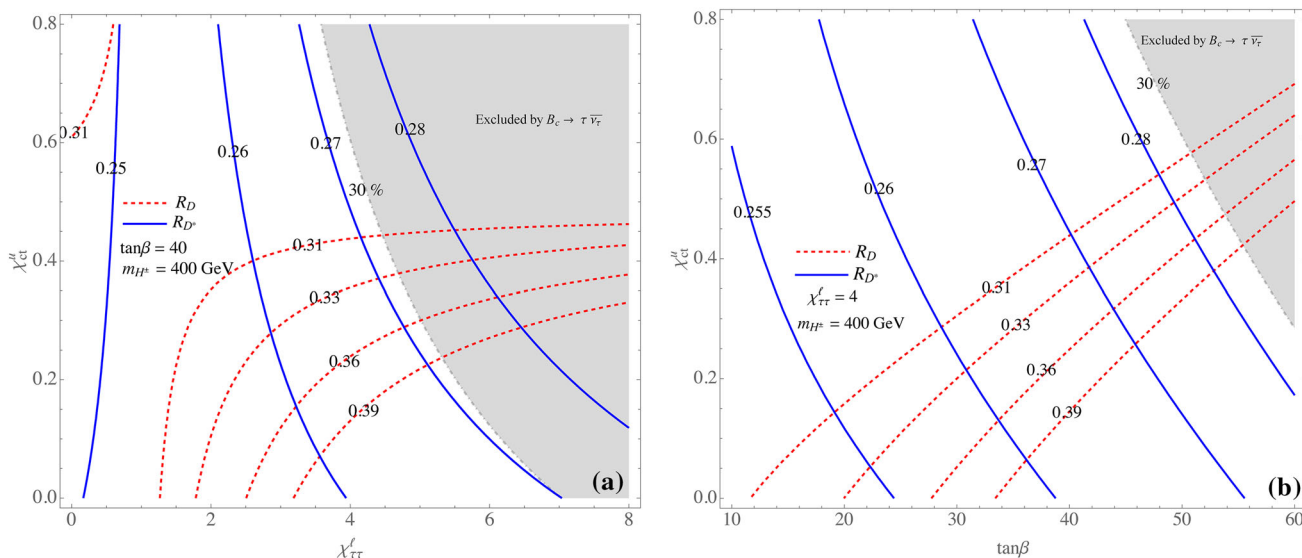
Fig. 2 The legend is the same as that in Fig. 1, and the upper limit of $BR(B_c \to \tau\bar{\nu}_\tau) < 30\%$ is included

respectively, and $m_{H^\pm} = 400$ GeV in both plots is used. For clarity, we use two limits, $\chi_{ct}^u = 0$ and $\chi_{\tau\tau}^\ell = 0$, to concretely show their importance in the following discussions. With $\chi_{ct}^u = 0$, we obtain $R_{D^*} \sim 0.3$ when $\chi_{\tau\tau}^\ell \sim 15$; however, the corresponding value of R_D has been larger than 1. In such case, the values of C_R^τ and C_L^τ are: $C_R^\tau \sim 1.79 \gg C_L^\tau \sim 0$. Since $B^- \to D\tau\bar{\nu}_\tau$ is sensitive to $C_R^\tau + C_L^\tau$, when we require $R_{D^*} \sim 0.3$, it can be expected that R_D will be significantly enhanced. With $\chi_{\tau\tau}^\ell = 0$, we obtain $R_D \sim 0.35$ with $\chi_{ct}^u \sim 1$, but $R_{D^*} \sim 0.24$, where $C_{R,L}^\tau \sim (-0.13, 0.24)$, which disfavors the earlier conclusion with $C_R^\tau > 0$ and $C_L^\tau < 0$. Based on these two limits, it is clear that neither χ_{ct}^u nor $\chi_{\tau\tau}^\ell$ can singly resolve the R_D and R_{D^*} anomalies at the same time. From Fig. 1(a), it can be seen that by properly adjusting both χ_{ct}^u and $\chi_{\tau\tau}^\ell$, the R_D and R_{D^*} excesses can be explained together.

In addition to the $B^- \to D^{(*)}\tau\bar{\nu}_\tau$ decay, the effective Hamiltonian in Eq. (11) also contributes to the $B_c \to \tau\bar{\nu}_\tau$ process [52,53], where the allowed upper limit, which is obtained from the difference between the SM prediction and the experimental measurement in B_c meson lifetime, is $BR(B_c^- \to \tau\bar{\nu}_\tau) < 30\%$ [53]. We express the BR for $B_c \to \tau\bar{\nu}_\tau$ as [53]

$$BR(B_c \to \tau\bar{\nu}_\tau) = \tau_{B_c} \frac{m_{B_c} m_\tau^2 f_{B_c}^2 G_F^2 |V_{cb}|^2}{8\pi} \left(1 - \frac{m_\tau^2}{m_{B_c}^2}\right)^2$$
$$\times \left|1 + \frac{m_{B_c}^2}{m_\tau(m_b + m_c)} \epsilon_P\right|^2, \quad (40)$$

where f_{B_c} is the B_c decay constant, $\epsilon_P = C_R^\tau - C_L^\tau$, and the SM result is $BR^{\mathrm{SM}}(B_c \to \tau\bar{\nu}_\tau) \approx 2.2\%$. As pointed

out by the authors in Refs. [52,53], due to the enhancement factor $m_{B_c}^2/m_\tau(m_b + m_c) \sim 3.6$, the obtained upper limit on $BR(B_c \to \tau\bar{\nu}_\tau)$ will exclude most of the parameter space for $R_{D^*} > R_{D^*}^{\mathrm{SM}}$. In order to demonstrate the strict constraint, we show the contours for $BR(B_c \to \tau\bar{\nu}_\tau)$ and $R_{D^{(*)}}$ in Fig. 2, where the gray area is excluded by the upper limit of $BR(B_c^- \to \tau\bar{\nu}_\tau)$. It can be clearly seen that when the constraint from $B_c \to \tau\bar{\nu}_\tau$ is included, $R_D \sim 0.39$ is still allowed; however, R_{D^*} becomes less than 0.28 when $\tan\beta = 40$ is used. Since R_{D^*} is limited by the $B_c \to \tau\bar{\nu}_\tau$ constraint, hereafter, we just show the range of $R_{D^*} = [0.25, 0.27]$.

4.3 τ polarization and FBA

The Belle collaboration recently reported the measurement of τ polarization in the $\bar{B} \to D^*\tau\bar{\nu}_\tau$ decay. If the R_D and R_{D^*} excesses originate from the new physics, the τ polarization can also be influenced. To understand the charged-Higgs contributions, according to Eq. (31), we plot the contours for P_D^τ (dashed) and $P_{D^*}^\tau$ (solid) as a function of χ_{ct}^u and $\chi_{\tau\tau}^\ell$ with $\tan\beta = 40$ in Fig. 3a, and the dependence of χ_{ct}^u and $\tan\beta$ with $\chi_{\tau\tau}^\ell = 4$ is shown in Fig. 3b, where the bounded areas denote the ranges of $R_D = [0.31, 0.39]$ (red) and $R_{D^*} = [0.25, 0.27]$ (blue). From the numerical analysis, it can be seen that P_D^τ and $P_{D^*}^\tau$ are more sensitive to χ_{ct}^u and $\chi_{\tau\tau}^\ell$, and they can be enhanced from 0.3 to 0.5 and ~ -0.5 to ~ -0.41, respectively.

Finally, we show the numerical results for the FBA. Since the τ lepton FBAs have not yet been observed, to demonstrate the charged-Higgs contributions, we adopt the integrated FBAs, which are defined by
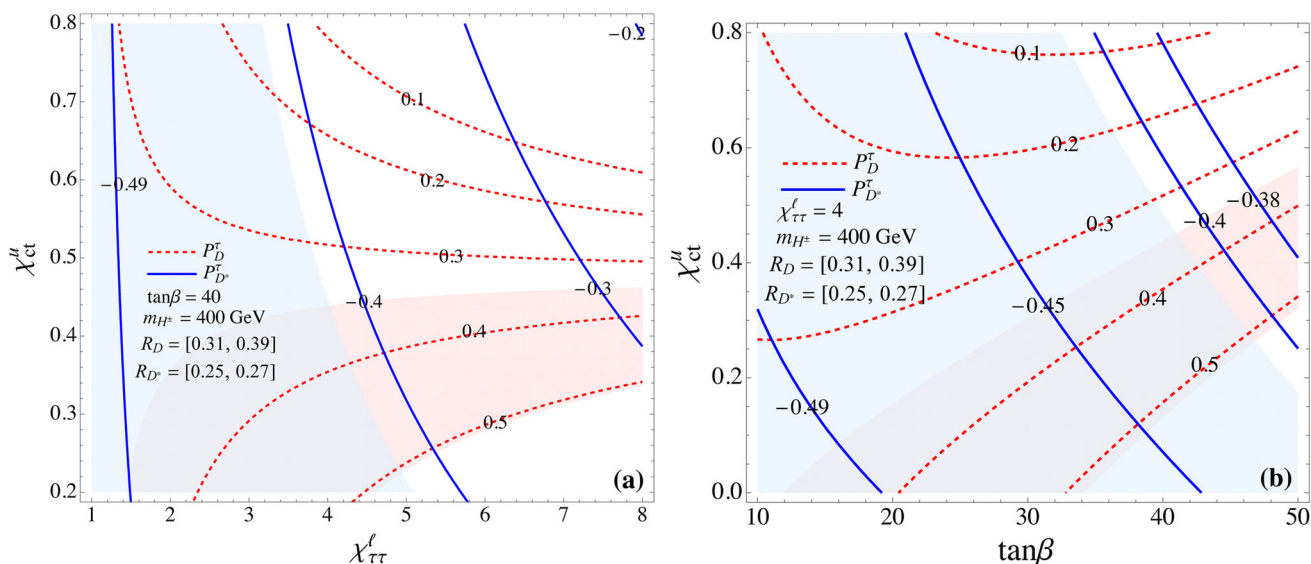
Fig. 3 Contours for P_D^τ (dashed) and $P_{D^*}^\tau$ (solid) as a function of χ_{ct}^u and **a** $\chi_{\tau\tau}^\ell$ with $\tan\beta = 40$, **b** $\tan\beta$ with $\chi_{\tau\tau}^\ell = 4$, where we have fixed $m_{H^\pm} = 400$ GeV. The bounded areas denote the ranges of $R_D = [0.31, 0.39]$ (red) and $R_{D^*} = [0.25, 0.27]$ (blue)
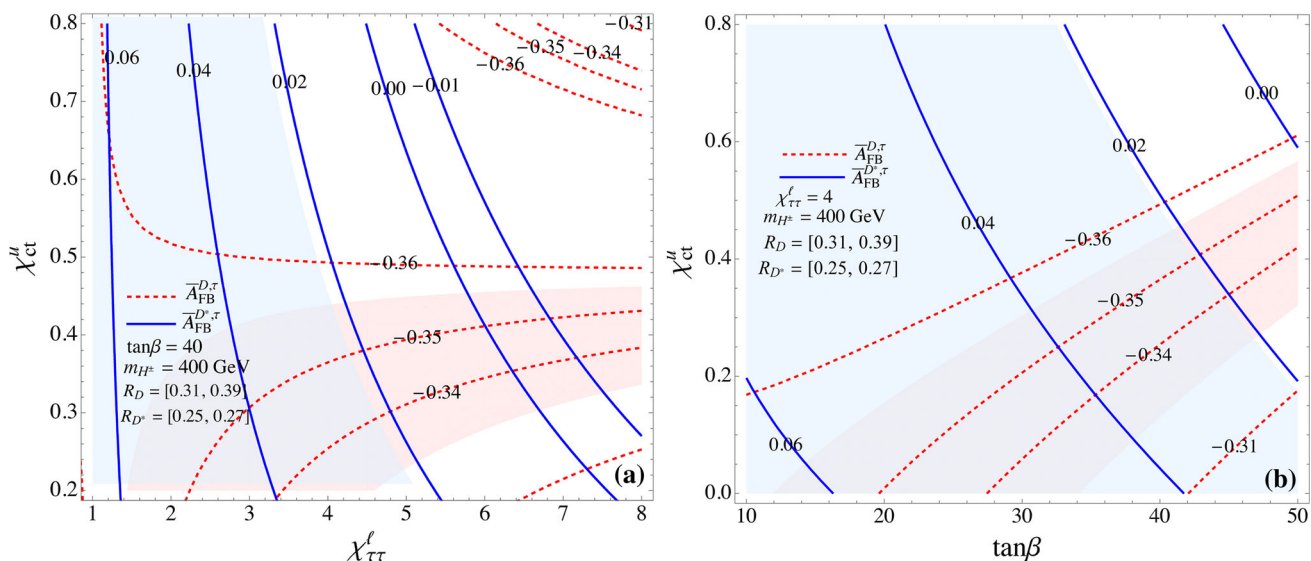

Fig. 4 The legend is the same as that in Fig. 3, but for FBA, defined in Eq. (41)

$$
\bar{A}_{FB}^{D,\tau} = -\frac{\int_{m_\tau^2}^{(m_B-m_D)^2} dq^2 \left(2m_\tau^2 \lambda_D \beta_\tau^4 F_1 X_D^{0\tau}\right)}{\int_{m_\tau^2}^{(m_B-m_D)^2} dq^2 \sqrt{\lambda_D}\beta_\tau^4 (H_D^+ + H_D^-)},
$$

$$
\bar{A}_{FB}^{D^*,\tau} = \frac{\int_{m_\tau^2}^{(m_B-m_{D^*})^2} dq^2 \sqrt{\lambda_{D^*}}\beta_\tau^4 \left(-2m_\tau \frac{\sqrt{\lambda_{D^*}}}{\sqrt{q^2}} h_{D^*}^0 X_{D^*}^{0\tau} + 4q^2 \sqrt{\lambda_{D^*}} A_1 V\right)}{\int_{m_\tau^2}^{(m_B-m_{D^*})^2} dq^2 \sqrt{\lambda_{D^*}}\beta_\tau^4 \sum_{\lambda=L,\pm}(H_{D^*}^{\lambda,+} + H_{D^*}^{\lambda,-})}.
$$

(41)

The contours for $\bar{A}_{FB}^{D,\tau}$ and $\bar{A}_{FB}^{D^*,\tau}$ as a function of χ_{ct}^u and $\chi_{\tau\tau}^\ell$ with $\tan\beta = 40$ are shown in Fig. 4a, whereas the contours with $\chi_{\tau\tau}^\ell = 4$ as a function of χ_{ct}^u and $\tan\beta$ are given in Fig. 4b. From the plots, it can be seen that $\bar{A}_{FB}^{D^*,\tau}$ is more

sensitive to the charged Higgs effects. The sign of $\bar{A}_{FB}^{D^*,\tau}$ in general can be changed in different parameter space; however, when the $BR(B_c \to \tau\bar{\nu}_\tau)$ constraint is included, its sign can be only positive. Moreover, the magnitude of $\bar{A}_{FB}^{D^*,\tau}$ is smaller than that of $\bar{A}_{FB}^{D,\tau}$. These behaviors can be understood from Eq. (41), in which the first and second terms in the numerator are opposite in sign and are from the D^* longitudinal and transverse parts, respectively. Although the first term is proportional to m_ℓ, when $m_\ell = m_\tau$, the contribution from the first becomes compatible with that of the second so that the sign can be flipped. The results with some chosen benchmarks of $(\chi_{ct}^u, \chi_{\ell\ell}^\ell)$ are given in Table 1. For comparisons, we also show the values of R_D, R_{D^*}, P_D^τ, and $P_{D^*}^\tau$ in the table.

Table 1 Values of integrated FBA, $R_{D(D^*)}$, and $P^\tau_{D(D^*)}$ with and without charged-Higgs effects in some chosen benchmarks of $(\chi^u_{ct}, \chi^\ell_{\ell\ell})$, where we have fixed $m_{H^\pm} = 400$ GeV and $\tan\beta = 40$

$(\chi^u_{ct}, \chi^\ell_{\tau\tau})$	$(0, 0)$	$(0.2, 3)$	$(0.2, 4)$	$(0.3, 3)$	$(0.3, 4)$
$\bar{A}^{D,\tau}_{FB}$	-0.359	-0.344	-0.335	-0.350	-0.344
$\bar{A}^{D^*,\tau}_{FB}$	0.064	0.043	0.033	0.040	0.029
R_D	0.306	0.364	0.396	0.343	0.362
R_{D^*}	0.257	0.264	0.268	0.266	0.270
P^τ_D	0.324	0.432	0.479	0.396	0.429
$P^\tau_{D^*}$	-0.500	-0.459	-0.438	-0.453	-0.428

5 Summary

We studied the charged-Higgs $H^\pm$ effects on the $\bar{B} \to (D, D^*)\ell\bar{\nu}_\ell$ decays in a generic two-Higgs-doublet model. In order to parametrize the new $H^\pm$ Yukawa couplings to the quarks and leptons, we employ the Cheng–Sher ansatz. Accordingly, the third-generation b-quark and τ-lepton related processes are dominant and can then be enhanced using a scheme with large $\tan\beta$. Based on this study, it can be seen that two parameters (χ^u_{ct} & $\chi^\ell_{\tau\tau}$) are required to explain the R_D and R_{D^*} excesses. However, when the constraint from the $B_c \to \tau\bar{\nu}_\tau$ decay with $BR(B_c \to \tau\bar{\nu}_\tau) < 30\%$ is applied, R_D can be still significantly enhanced while R_{D^*} can only have a slight change. The τ polarizations in the $\bar{B} \to (D, D^*)\tau\bar{\nu}_\tau$ decays were calculated, and it was found that they are sensitive to the $H^\pm$ effects. The integrated τ-lepton forward–backward asymmetries were studied. We found that the asymmetry of $\bar{B} \to D^*\tau\bar{\nu}_\tau$ is more sensitive to the $H^\pm$ effects. Although the sign of $\bar{A}^{D^*,\tau}_{FB}$ can be reversed in some parameter space, when the constraint from $B_c \to \tau\bar{\nu}_\tau$ is included, the sign is only positive.

Appendix

In order to derive the charged lepton-helicity amplitudes in the $\bar{B} \to M\ell\bar{\nu}_\ell$ decay, we need the specific spinor states of a charged lepton and neutrino in the q^2 rest frame. Let $p = (E, \vec{p})$ be the four-momentum of a spin-1/2 particle, the solutions of the Dirac equation for positive and negative energy are expressed as

$$u_\pm(p) = \frac{1}{\sqrt{E+m}}\begin{pmatrix} \sqrt{E+m}\,\chi_\pm(\vec{p}) \\ \vec{\sigma}\cdot\vec{p}\,\chi_\pm(\vec{p}) \end{pmatrix},$$

$$v_\pm(p) = \frac{1}{\sqrt{E+m}}\begin{pmatrix} \vec{\sigma}\cdot\vec{p}\,\chi_\mp(\vec{p}) \\ \sqrt{E+m}\,\chi_\mp(\vec{p}) \end{pmatrix}, \quad (42)$$

where the $\pm$ indices in χ are the eigenvalues of $\vec{\sigma}\cdot\vec{p}/|\vec{p}|$, and $+/-$ denote the left-/right-handed states, respectively. If the spatial momentum of a particle is taken as $\vec{p} = p(\sin\theta\cos\phi, \sin\theta\sin\phi, \cos\theta)$, the eigenstates of $\vec{\sigma}\cdot\vec{p}$ can be found to be

$$\chi_+(\vec{p}) = \begin{pmatrix} \cos\frac{\theta}{2} \\ e^{i\phi}\sin\frac{\theta}{2} \end{pmatrix}, \quad \chi_-(\vec{p}) = \begin{pmatrix} \sin\frac{\theta}{2} \\ -e^{i\phi}\cos\frac{\theta}{2} \end{pmatrix}. \quad (43)$$

With the Pauli–Dirac representation of the γ-matrices, which are defined by

$$\gamma^0 = \begin{pmatrix} \mathbf{1} & 0 \\ 0 & -\mathbf{1} \end{pmatrix}, \quad \gamma^i = \begin{pmatrix} 0 & \sigma^i \\ -\sigma^i & 0 \end{pmatrix}, \quad \gamma_5 = \gamma^5 = \begin{pmatrix} 0 & \mathbf{1} \\ \mathbf{1} & 0 \end{pmatrix}, \quad (44)$$

we get $\bar{\ell}_{u_\pm}[...](1-\gamma_5)v_{v_+} = 2\bar{\ell}_{u_\pm}[...]v_{v_+}$ and $\bar{\ell}[...](1-\gamma_5)v_{v_+} = 0$ when $m_\nu = 0$ is applied, in which $[...] = \{1, \gamma^\mu, \sigma^{\mu\nu}\}$.

For simplifying the derivations of $\bar{\ell}_{u_\pm}[...](1-\gamma_5)v_{v_+}$, we define some useful polarization vectors:

$$|\vec{P}|\epsilon^\mu_X \equiv P^\mu - \frac{P\cdot q}{q^2}q^\mu, \quad \epsilon^\mu_X\epsilon_{X\mu} = -1,$$

$$\frac{E_{D^*}}{m_{D^*}}\epsilon^\mu_Z \equiv \epsilon^\mu(L) - \frac{\epsilon\cdot q}{q^2}q^\mu, \quad \sqrt{\frac{\lambda_{D^*}}{2}}e^\mu_{D^*}(T) \equiv \varepsilon^{\mu\nu\rho\sigma}\epsilon_\nu(T)P_\rho q_\sigma \quad (45)$$

with $|\vec{P}| = \sqrt{\lambda_M}/\sqrt{q^2}$. According to the chosen coordinates in the q^2 rest frame, the leptonic current associated with a specific charged lepton helicity can be derived as follows: for the $B \to D$ case, we get

$$\bar{\ell}_{u_+}\not\!\epsilon_X(1-\gamma_5)v_{v_+} = 2m_\ell\beta_\ell\cos\theta_\ell,$$

$$\bar{\ell}_{u_+}(1-\gamma_5)v_{v_+} = -2\sqrt{q^2}\beta_\ell,$$

$$\bar{\ell}_{u_-}\not\!\epsilon_X(1-\gamma_5)v_{v_+} = -2\sqrt{q^2}\beta_\ell\sin\theta_\ell,$$

$$\bar{\ell}_{u_-}(1-\gamma_5)v_{v_+} = 0 \quad (46)$$

with $\beta_\ell = \sqrt{1 - m^2_\ell/q^2}$. For the $B \to D^*$ case, the D^* longitudinal parts are obtained:

$$\bar{\ell}_{u_+}\not\!\epsilon_Z(1-\gamma_5)v_{v_+} = 2m_\ell\beta_\ell\cos\theta_\ell, \quad (47)$$

$$\bar{\ell}_{u_-}\not\!\epsilon_Z(1-\gamma_5)v_{v_+} = -2\sqrt{q^2}\beta_\ell\sin\theta_\ell, \quad (48)$$

while the two D^* transverse parts are, respectively, given by

$$\bar{\ell}_{u_+}\slashed{\epsilon}_{D^*}(T)(1-\gamma_5)v_{v_+} = -2m_\ell\beta_\ell \begin{cases} \frac{i}{\sqrt{2}}\sin\theta_\ell e^{-i\phi} & (T=+), \\ \frac{i}{\sqrt{2}}\sin\theta_\ell e^{i\phi} & (T=-), \end{cases} \tag{49}$$

$$\bar{\ell}_{u_-}\slashed{\epsilon}_{D^*}(T)(1-\gamma_5)v_{v_+}$$
$$= -2\sqrt{q^2}\beta_\ell \begin{cases} \frac{-i}{\sqrt{2}}(1-\cos\theta_\ell)e^{-i\phi} & (T=+), \\ \frac{i}{\sqrt{2}}(1+\cos\theta_\ell)e^{i\phi} & (T=-). \end{cases} \tag{50}$$

The differential decay rates shown in Eq. (28) are functions of q^2 and θ_ℓ. After integrating out the polar angle, the differential decay rate with each lepton helicity as a function of q^2 can be obtained as follows: For the $\bar{B} \to D\ell\bar{\nu}_\ell$ decay, they can be shown:

$$\frac{d\Gamma_D^{h=\pm}}{dq^2} = \frac{G_F^2|V_{cb}|^2\sqrt{\lambda_D}\beta_\ell^4}{256\pi^3 m_B^3}H_D^\pm, \tag{51}$$

$$H_D^+ = \frac{2m_\ell^2}{3q^2}\lambda_D F_1^2 + 2m_\ell^2 q^2|X_D^0|^2, \quad H_D^- = \frac{4}{3}\lambda_D F_1^2; \tag{52}$$

and for the $\bar{B} \to D^*\ell\nu_\ell$ decay, they are expressed as

$$\frac{d\Gamma_{D^*}^{\lambda,h=\pm}}{dq^2} = \frac{G_F^2|V_{cb}|^2\sqrt{\lambda_{D^*}}\beta_\ell^4}{256\pi^3 m_B^3}H_{D^*}^{\lambda,\pm}, \tag{53}$$

$$H_{D^*}^{L,+} = \frac{2m_\ell^2}{3}|h_{D^*}^0|^2 + \frac{2m_\ell^2}{q^2}\lambda_{D^*}|X_{D^*}^0|^2, \quad H_{D^*}^{L,-} = \frac{4q^2}{3}|h_{D^*}^0|^2, \tag{54}$$

$$H_{D^*}^{T=\pm,+} = \frac{2m_\ell^2}{3}|h_{D^*}^\pm|^2, \quad H_{D^*}^{T=\pm,-} = \frac{4q^2}{3}|h_{D^*}^\pm|^2. \tag{55}$$

References

1. J.P. Lees et al., BaBar collaboration. Phys. Rev. Lett. **109**, 101802 (2012). arXiv:1205.5442 [hep-ex]
2. J. P. Lees et al., BaBar collaboration, Phys. Rev. D **88**(7), 072012 (2013). arXiv:1303.0571 [hep-ex]
3. M. Huschle et al., Belle collaboration, Phys. Rev. D **92**(7), 072014 (2015). arXiv:1507.03233 [hep-ex]
4. A. Abdesselam et al., Belle collaboration, arXiv:1603.06711 [hep-ex]
5. S. Hirose et al., Belle collaboration, arXiv:1612.00529 [hep-ex]
6. R. Aaij et al., LHCb collaboration, Phys. Rev. Lett. **115**(11), 111803 (2015) **(Addendum: [Phys. Rev. Lett. 115, no. 15, 159901 (2015)])** arXiv:1506.08614 [hep-ex]
7. Y. Amhis et al., arXiv:1612.07233 [hep-ex]
8. J. A. Bailey et al., MILC collaboration, Phys. Rev. D **92**(3), 034506 (2015) arXiv:1503.07237 [hep-lat]
9. H. Na et al., HPQCD collaboration, Phys. Rev. D **92**(5), 054510 (2015) **(Erratum: [Phys. Rev. D 93, no. 11, 119906 (2016)])** arXiv:1505.03925 [hep-lat]
10. S. Fajfer, J.F. Kamenik, I. Nisandzic, Phys. Rev. D **85**, 094025 (2012). arXiv:1203.2654 [hep-ph]
11. S. Fajfer, J.F. Kamenik, I. Nisandzic, J. Zupan, Phys. Rev. Lett. **109**, 161801 (2012). arXiv:1206.1872 [hep-ph]
12. A. Crivellin, C. Greub, A. Kokulu, Phys. Rev. D **86**, 054014 (2012). arXiv:1206.2634 [hep-ph]
13. A. Datta, M. Duraisamy, D. Ghosh, Phys. Rev. D **86**, 034027 (2012). arXiv:1206.3760 [hep-ph]
14. J.A. Bailey et al., Phys. Rev. Lett. **109**, 071802 (2012). arXiv:1206.4992 [hep-ph]
15. N.G. Deshpande, A. Menon, JHEP **1301**, 025 (2013). arXiv:1208.4134 [hep-ph]
16. A. Celis, M. Jung, X.Q. Li, A. Pich, JHEP **1301**, 054 (2013). arXiv:1210.8443 [hep-ph]
17. X. G. He, G. Valencia, Phys. Rev. D **87**(1), 014014 (2013) arXiv:1211.0348 [hep-ph]
18. M. Tanaka, R. Watanabe, Phys. Rev. D **87**(3), 034028 (2013) arXiv:1212.1878 [hep-ph]
19. P. Ko, Y. Omura, C. Yu, JHEP **1303**, 151 (2013). arXiv:1212.4607 [hep-ph]
20. P. Biancofiore, P. Colangelo, F. De Fazio, Phys. Rev. D **87**(7), 074010 (2013) arXiv:1302.1042 [hep-ph]
21. I. Dorsner, S. Fajfer, N. Kosnik, I. Nisandzic, JHEP **1311**, 084 (2013). arXiv:1306.6493 [hep-ph]
22. Y. Sakaki, M. Tanaka, A. Tayduganov, R. Watanabe, Phys. Rev. D **88**(9), 094012 (2013) arXiv:1309.0301 [hep-ph]
23. A. Abada, A.M. Teixeira, A. Vicente, C. Weiland, JHEP **1402**, 091 (2014). arXiv:1311.2830 [hep-ph]
24. R. Alonso, B. Grinstein, J. Martin Camalich, JHEP **1510**, 184 (2015) arXiv:1505.05164 [hep-ph]
25. A. Greljo, G. Isidori, D. Marzocca, JHEP **1507**, 142 (2015). arXiv:1506.01705 [hep-ph]
26. L. Calibbi, A. Crivellin, T. Ota, Phys. Rev. Lett. **115**, 181801 (2015). arXiv:1506.02661 [hep-ph]
27. M. Freytsis, Z. Ligeti, J. T. Ruderman, Phys. Rev. D **92**(5), 054018 (2015) arXiv:1506.08896 [hep-ph]
28. A. Crivellin, J. Heeck, P. Stoffer, Phys. Rev. Lett. **116**(8), 081801 (2016) arXiv:1507.07567 [hep-ph]
29. S. Bhattacharya, S. Nandi, S. K. Patra, Phys. Rev. D **93**(3), 034011 (2016) arXiv:1509.07259 [hep-ph]
30. M. Bauer, M. Neubert, Phys. Rev. Lett. **116**(14), 141802 (2016) arXiv:1511.01900 [hep-ph]
31. C. Hati, G. Kumar, N. Mahajan, JHEP **1601**, 117 (2016). arXiv:1511.03290 [hep-ph]
32. S. Fajfer, N. Kosnik, Phys. Lett. B **755**, 270 (2016). arXiv:1511.06024 [hep-ph]
33. R. Barbieri, G. Isidori, A. Pattori, F. Senia, Eur. Phys. J. C **76**(2), 67 (2016) arXiv:1512.01560 [hep-ph]
34. J. Zhu, H. M. Gan, R. M. Wang, Y. Y. Fan, Q. Chang, Y. G. Xu, Phys. Rev. D **93**(9), 094023 (2016) arXiv:1602.06491 [hep-ph]
35. R. Alonso, A. Kobach, J. Martin Camalich, Phys. Rev. D **94**(9), 094021 (2016) arXiv:1602.07671 [hep-ph]
36. S.M. Boucenna, A. Celis, J. Fuentes-Martin, A. Vicente, J. Virto, Phys. Lett. B **760**, 214 (2016). arXiv:1604.03088 [hep-ph]
37. D. Das, C. Hati, G. Kumar, N. Mahajan, Phys. Rev. D **94**, 055034 (2016). arXiv:1605.06313 [hep-ph]
38. F. Feruglio, P. Paradisi, A. Pattori, Phys. Rev. Lett. **118**(1), 011801 (2017) arXiv:1606.00524 [hep-ph]
39. G. Cvetic, C. S. Kim, Phys. Rev. D **94**(5), 053001 (2016) **(Erratum: [Phys. Rev. D 95, no. 3, 039901 (2017)])** arXiv:1606.04140 [hep-ph]
40. M. A. Ivanov, J. G. Korner, C. T. Tran, Phys. Rev. D **94**(9), 094028 (2016) arXiv:1607.02932 [hep-ph]
41. S.M. Boucenna, A. Celis, J. Fuentes-Martin, A. Vicente, J. Virto, JHEP **1612**, 059 (2016). arXiv:1608.01349 [hep-ph]
42. N. G. Deshpande, X. G. He, Eur. Phys. J. C **77**(2), 134 (2017) arXiv:1608.04817 [hep-ph]

43. D. Becirevic, S. Fajfer, N. Kosnik, O. Sumensari, Phys. Rev. D **94**(11), 115021 (2016) arXiv:1608.08501 [hep-ph]
44. S. Sahoo, R. Mohanta, A. K. Giri, Phys. Rev. D **95**(3), 035027 (2017) arXiv:1609.04367 [hep-ph]
45. B. Bhattacharya, A. Datta, J.P. Guevin, D. London, R. Watanabe, JHEP **1701**, 015 (2017). arXiv:1609.09078 [hep-ph]
46. G. Hiller, D. Loose, K. Schonwald, JHEP **1612**, 027 (2016). arXiv:1609.08895 [hep-ph]
47. D. Bardhan, P. Byakti, D. Ghosh, JHEP **1701**, 125 (2017). arXiv:1610.03038 [hep-ph]
48. L. Wang, J. M. Yang, Y. Zhang, arXiv:1610.05681 [hep-ph]
49. X.Q. Li, Y.D. Yang, X. Zhang, JHEP **1702**, 068 (2017). arXiv:1611.01635 [hep-ph]
50. S. Bhattacharya, S. Nandi, S. K. Patra, arXiv:1611.04605 [hep-ph]
51. R. Barbieri, C. W. Murphy, F. Senia, Eur. Phys. J. C **77**(1), 8 (2017) arXiv:1611.04930 [hep-ph]
52. X.Q. Li, Y.D. Yang, X. Zhang, JHEP **1608**, 054 (2016). arXiv:1605.09308 [hep-ph]
53. R. Alonso, B. Grinstein, J. Martin Camalich, Phys. Rev. Lett. **118**(8), 081802 (2017) arXiv:1611.06676 [hep-ph]
54. A. Celis, M. Jung, X. Q. Li, A. Pich, arXiv:1612.07757 [hep-ph]
55. M. A. Ivanov, J. G. Korner, C. T. Tran, Phys. Rev. D **95**(3), 036021 (2017) arXiv:1701.02937 [hep-ph]
56. M. Wei, Y. Chong-Xing, Phys. Rev. D **95**(3), 035040 (2017) arXiv:1702.01255 [hep-ph]
57. G. Cvetic, F. Halzen, C. S. Kim, S. Oh, arXiv:1702.04335 [hep-ph]
58. C. H. Chen, T. Nomural, H. Okada, arXiv:1703.03251 [hep-ph]
59. J. Hernandez-Sanchez, S. Moretti, R. Noriega-Papaqui, A. Rosado, JHEP **1307**, 044 (2013). arXiv:1212.6818 [hep-ph]
60. R. Benbrik, C. H. Chen, T. Nomura, Phys. Rev. D **93**(9), 095004 (2016) arXiv:1511.08544 [hep-ph]
61. A. Arhrib, R. Benbrik, C. H. Chen, M. Gomez-Bock, S. Semlali, Eur. Phys. J. C **76**,(6), 328 (2016) arXiv:1508.06490 [hep-ph]
62. M. Tanaka, R. Watanabe, Phys. Rev. D **82**, 034027 (2010). arXiv:1005.4306 [hep-ph]
63. T.P. Cheng, M. Sher, Phys. Rev. D **35**, 3484 (1987)
64. J. Kalinowski, Phys. Lett. B **245**, 201 (1990)
65. R. Garisto, Phys. Rev. D **51**, 1107 (1995). arXiv:hep-ph/9403389
66. C.H. Chen, C.Q. Geng, Phys. Rev. D **71**, 077501 (2005). arXiv:hep-ph/0503123
67. C.H. Chen, C.Q. Geng, JHEP **0610**, 053 (2006). arXiv:hep-ph/0608166
68. Y.H. Ahn, C.H. Chen, Phys. Lett. B **690**, 57 (2010). arXiv:1002.4216 [hep-ph]
69. R. Alonso, J. Martin Camalich, S. Westhoff, Phys. Rev. D **95**(9), 093006 (2017) arXiv:1702.02773 [hep-ph]
70. I. Caprini, L. Lellouch, M. Neubert, Nucl. Phys. B **530**, 153 (1998). arXiv:hep-ph/9712417
71. F. U. Bernlochner, Z. Ligeti, M. Papucci, D. J. Robinson, arXiv:1703.05330 [hep-ph]
72. D. Melikhov, B. Stech, Phys. Rev. D **62**, 014006 (2000). arXiv:hep-ph/0001113
73. C. Patrignani et al., Particle data group. Chin. Phys. C **40**, 100001 (2016)